Available online at www.sciencedirect.com
ScienceDirect
Catalysis Today 137 (2008) 362–366
CATALYSIS TODAY
www.elsevier.com/locate/cattod

The role of support on the performance of platinum-based catalysts for the total oxidation of polycyclic aromatic hydrocarbons

Edwin Ntainjua N., Albert F. Carley, Stuart H. Taylor *

Cardiff University, School of Chemistry, Main Building, Park Place, Cardiff CF10 3AT, UK

Available online 26 December 2007

Abstract

A range of Pt supported catalysts have been evaluated for the total oxidation of naphthalene. Catalysts contained 0.5 wt% Pt on a range of supports (γ-Al_2O_3, TiO_2, SiO_2, SnO_2, and CeO_2). SiO_2 was the best support, the 0.5%Pt/SiO_2 catalyst showing a conversion to carbon dioxide of over 90% at 200 °C (100 vppm naphthalene, GHSV = 45,000 h^{-1}). The catalyst also showed a considerably higher activity (in the temperature range 100–175 °C) than a CeO_2 catalyst recently reported to be one of the most effective catalysts for the total oxidation of naphthalene. The high activity of the 0.5%Pt/SiO_2 catalyst has been attributed to the relatively low dispersion and relatively large size of Pt particles. Furthermore, due to the acidic and non-reducible nature of the SiO_2, platinum is expected to have a weak interaction with the support. XPS data identified the presence of Pt^0 on the surface and this contributes to the high activity.
© 2007 Elsevier B.V. All rights reserved.

Keywords: Catalytic oxidation; Support; Pt; Naphthalene; PAHs; XPS

1. Introduction

Polycyclic aromatic hydrocarbons (PAHs) have been cited as carcinogenic and environmentally hazardous substances. They result predominantly from the incomplete combustion of organic matter [1–4]. PAH emissions have been linked to serious risks to health and stringent limits on their discharge have been imposed. The Comite Europeen de Normalisation has for instance suggested an emission standard of 2500, 100, and 150 mg Nm^{-3} for CO, total hydrocarbons, and particulate matters from boilers and wood stoves, for a fuel supply of 50–150 KW [5]. Catalytic oxidation is so far one of the most economical and effective techniques for the destruction of volatile organic compounds and PAHs. Several research groups [6–14] have reported the use of metal oxide and supported metal catalysts for the total destruction of naphthalene (a model PAH). Amongst these catalysts, Pt/γ-Al_2O_3 [8,9] V-modified Pt/γ-Al_2O_3 [14], Pd-modified zeolites [10] and CeO_2 [13,15] have demonstrated the best activities for the total oxidation of naphthalene. In previous studies based on the use of Pt-supported or modified Pt-supported catalysts for PAH abatement, γ-Al_2O_3 has been employed as the support. However, various studies [16–20] have shown that other metal oxides, such as TiO_2, ZrO_2 and SnO_2, are better catalyst supports than γ-Al_2O_3 in the oxidation of hydrocarbons. In this work, we investigate, for the first time, the effect of a variety of supports (γ-Al_2O_3, TiO_2, SiO_2, SnO_2, and CeO_2) on the activity of Pt-supported catalysts in naphthalene oxidation. The activities of the synthesized Pt-supported catalysts are compared with that of a CeO_2 catalyst (prepared by homogeneous precipitation with urea) recently shown to be one of the best catalysts for naphthalene total oxidation [13,15].

2. Experimental

2.1. Catalyst preparation

Pt-supported catalysts were prepared by dissolving 0.0432 g of hexachloroplatinate(IV) hydrate (Aldrich, 99.9%) in 100 ml of deionised water. The solution was heated to 80 °C and stirred continuously. Three grams of the appropriate support; γ-Al_2O_3, TiO_2 (P 25, Degussa), SiO_2 (Matrex Silica 60 – Fischer Scientific Ltd., 99+%), Tin(IV) oxide (325 mesh, Aldrich, 99.9%) or cerium(IV) oxide (Aldrich, 99.9%) was then added to the heated solution and stirred at 80 °C to form a paste. This was then dried by evaporation at 100 °C and final catalysts were

* Corresponding author.
E-mail address: taylorsh@cf.ac.uk (S.H. Taylor).

0920-5861/$ – see front matter © 2007 Elsevier B.V. All rights reserved.
doi:10.1016/j.cattod.2007.10.116

Table 1
Catalyst characterisation results from nitrogen adsorption, powder X-ray diffraction and CO chemisorption

Catalyst	Surface area ($m^2\ g^{-1}$)	Crystaline phase	Pt surface area[a] ($m^2\ g^{-1}$)	Pt dispersion[a] (%)	Average particle size of Pt[a] (Å)
0.5%Pt/SiO_2	442	–	0.3	12	49
0.5%Pt/Al_2O_3	169	γ Al_2O_3, defect cubic spinel	1.3	52	10.9
0.5%Pt/TiO_2	44	TiO_2 (rutile and anatase, both tetragonal)	1.7	68	8.3
0.5%Pt/CeO_2	11	CeO_2, cubic fluorite	1.5	61	9.4
0.5%Pt/SnO_2	12	SnO_2	0.1	3	189
CeO_2 (U)	126	CeO_2, cubic fluorite	–	–	–

[a] By CO chemisorption analysis, 230 mg of catalyst, 40 °C.

obtained by calcination in static air at 550 °C for 6 h (heating rate of 10 °C min^{-1} and cooling in air). All Pt-supported catalysts had Pt loading of 0.5 wt%. A CeO_2 catalyst was prepared using a method of homogeneous precipitation with urea (CeO_2 (U)), similar to that reported previously [13].

2.2. Catalyst characterization

The surface areas of catalysts were determined by multi point N_2 adsorption at 77 K using the BET method and crystalline phases were identified by powder X-ray diffraction. CO chemisorption was performed using an Autosorb-1 Quantachrome equipment. For each analysis, the sample was first treated with He and H_2 prior to CO uptake. The sample was degassed by flowing He over the sample while heating to 120 °C (ramp = 20 °C min^{-1}). At 120 °C He was flowed for a further 30 min. The sample was then reduced with H_2 by heating to 400 °C. At 400 °C, the sample was treated with high purity H_2 for 2 h, before evacuating for 3 h to remove any physisorbed H_2. This was followed by CO chemisorption at 40 °C using high purity gas. XPS measurements were made on a Kratos Axis Ultra DLD spectrometer at Kratos Analytical, Manchester UK, using monochromatic Al K(radiation, and analyser pass energies of 160 eV (survey scans) or 40 eV (detailed scans). Binding energies are referenced to the C(1s) peak from adventitious carbonaceous contamination, assumed to have a binding energy of 284.7 eV.

2.3. Catalytic activity

Catalysts were tested in powdered form using a 1/4 in. o.d. stainless steel microreactor. The reaction feed was 100 vppm naphthalene in air, with a total flow rate of 50 ml min^{-1}. Catalysts were packed to a constant volume to give a gas hourly space velocity of 45 000 h^{-1} for all studies. Analysis was performed by an on-line gas chromatograph with thermal conductivity and flame ionization detectors. Catalytic activity was measured over the temperature range 100–300 °C in incremental steps, and temperatures were measured by a thermocouple placed in the catalyst bed. Once steady state operation was reached at each temperature a number of consistent analyses were obtained. Oxidation activity was expressed as yield of carbon dioxide [15].

3. Results and discussion

The BET surface areas for Pt-supported catalysts are shown in Table 1. Compared to the supports alone the surface area remained unchanged or decreased slightly after impregnation with Pt. The decrease in surface area corresponds to the filling of micro pores of the support. Apart from 0.5%Pt/SiO_2 and 0.5%Pt/Al_2O_3 which have relatively high surface areas (442 and 169 $m^2\ g^{-1}$, respectively), CeO_2 (U) has a higher surface area (126 $m^2\ g^{-1}$) than all of the other Pt-supported catalysts.

Table 1 also shows the crystalline phases of the catalysts determined from XRD. For catalysts with crystalline supports there was no discernable modification of the structure of the support on the addition of Pt. There was no evidence for diffraction from a Pt phase, which was not surprising considering the low loading and the expected relatively high dispersion. The XRD pattern of CeO_2 (U) was analogous to the pattern of the CeO_2 support and 0.5%Pt/CeO_2 catalyst, showing peaks corresponding to a cubic fluorite ceria phase. Ceria (prepared by homogeneous precipitation with urea) was less crystalline and crystallites were smaller compared to the ceria used as support, but it consisted of the same cubic fluorite structure. Laser Raman spectroscopy confirmed the XRD data as there was no detectable modification of the support on the addition of Pt. For example the Raman spectra of the ceria supported catalyst; ceria support and the ceria catalyst prepared by precipitation with urea showed the single characteristic ceria vibration at 462 cm^{-1} [13].

CO chemisorption results for the Pt-supported catalysts are shown in Table 1. The Pt surface area, Pt dispersion and the average size of Pt particles all varied as a function of the type of support. As expected there was a decrease in particle size and an increase in surface area of Pt as the Pt dispersion increased. The metal surface area, Pt dispersion and Pt particle size varied as a function of support in the order:

$$Pt/SnO_2 \quad Pt/SiO_2 \quad Pt/Al_2O_3 \quad Pt/CeO_2 \quad Pt/TiO_2$$
$$\rightarrow$$
Increasing Pt surface area
Increasing Pt dispersion
Decreasing Pt particle size

The activity results (Fig. 1) showed that CeO_2 (U) was more active than all other Pt-supported catalysts, except for 0.5%Pt/SiO_2 which showed a considerably higher activity than CeO_2

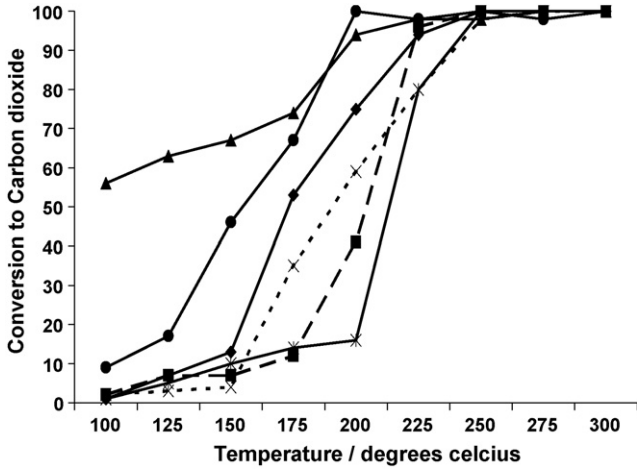

Fig. 1. Catalytic performance of Pt-supported catalysts and CeO_2 (U) in naphthalene total oxidation: (◆) 0.5%Pt/Al_2O_3; (■) 0.5%Pt/TiO_2; (▲) 0.5%Pt/SiO_2; (×) 0.5%Pt/SnO_2; (*) 0.5%Pt/CeO_2; (●) CeO_2 (U).

(U) in the temperature range 100–175 °C. This catalyst gave a CO_2 yield of over 50% at 100 °C and over 90% at 200 °C. The activities of the Pt catalysts investigated in this work decreased in the order:

$$Pt/SiO_2 > Pt/Al_2O_3 > Pt/SnO_2 > Pt/TiO_2 > Pt/CeO_2$$

0.5%Pt/SnO_2 was more active than 0.5%Pt/TiO_2 at low temperatures (100–175 °C) but showed considerably lower activity than the latter above 200 °C. The conversion of naphthalene over the supports was negligible below 250 °C, and therefore the presence of Pt is required to produce appreciable oxidation activity.

The catalytic performance of the best catalyst (0.5%Pt/SiO_2) in this work was evaluated for naphthalene oxidation in the temperature range of 100–300 °C in three consecutive cycles and as a function of time on stream for a period of 48 h. The catalytic performance remained unchanged throughout the three cycles and the catalyst maintained its high naphthalene conversion to CO_2 during the 48 h on stream.

In order to understand the relative activity of the different Pt catalyst it is necessary to consider a number of the features of the catalysts: these are the dispersion of the active metal, and associated properties such as metal particle size, and the nature of the interaction of the metal with the support. Firstly, it is noteworthy that the naphthalene oxidation activity of the Pt-supported catalysts varied in a similar order to properties relating to the active metal surface area. In particular, the activity of the catalysts showed a general decrease of activity as the Pt dispersion increased, *i.e.* particle size decreased (Fig. 2). Therefore, it appears that the high activity catalysts for naphthalene total oxidation require a lower dispersion and larger average active metal particle size. The correlation was not universal as 0.5%Pt/SnO_2 showed considerably lower naphthalene oxidation activity than Pt/SiO_2 and Pt/Al_2O_3 irrespective of the higher Pt particle size and the lower dispersion. The data suggest that there may be an optimum particle size for Pt in relation to naphthalene oxidation. However, the very low activity of the SnO_2 supported catalyst

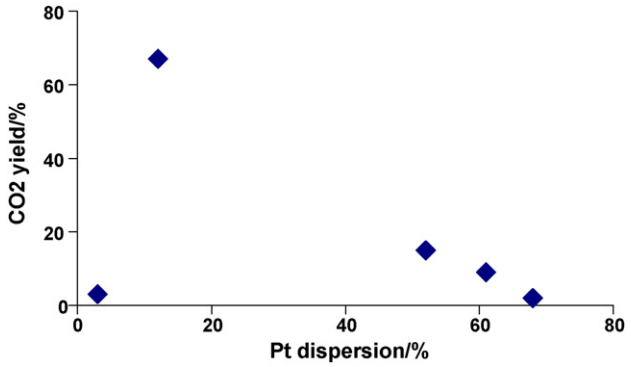

Fig. 2. The relationship between the activity for naphthalene total oxidation at 150 °C and the dispersion of Pt on different catalyst supports.

compared with the SiO_2 based catalyst suggests the influence of other factors, in addition to dispersion, are also important in determining catalyst activity. The very low Pt surface area and dispersion correspondingly very large Pt particle size of the catalyst supported on SnO_2 is not surprising. The SnO_2 support is hydrophobic and impregnation with an aqueous Pt salt solution during catalyst preparation would lead to large metal particles as the catalyst dries, due to poor wetting of the support surface.

Fig. 3 shows the relationship between naphthalene total oxidation expressed in terms of turnover frequency (TOF) and Pt particle size on the different supports. Interestingly, the TOF increases as the Pt particle size increases, to a maximum for Pt/SiO_2 and then decreased for the Pt/SnO_2 catalyst with the largest Pt particle size. It is clear that generally larger average Pt particle sizes had a greater TOF than smaller Pt particles and are therefore more efficient for naphthalene total oxidation. Initially this may be counterintuitive, as often activity is greater with catalysts with increased dispersion. However, naphthalene is a relatively large molecule compared with many of the reactants previously investigated on Pt based catalysts, and the larger particle size is required for adsorption and oxidation to take place.

Although there is a clear relationship between the active Pt surface area, dispersion and average particle size and catalyst activity it is not a simple one. Close inspection of the activity data (Fig. 1) shows that the general order of activity can change

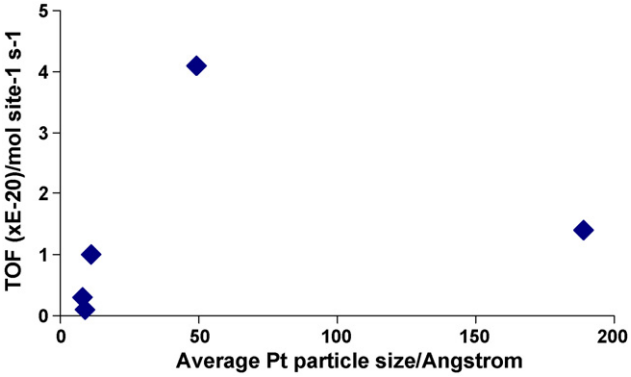

Fig. 3. Relationship between turnover frequency for naphthalene total oxidation at 175 °C and average Pt particle size.

under specific circumstances. This is not surprising considering the diverse nature of the supports employed. Strong metal-support interactions (SMSI) have been reported to account for the activity and selectivity of supported metal catalysts [21], and the nature of this metal support interaction (MSI) was found to depend on the nature of the support. Whilst CeO_2 is known to interact very strongly with Pt [22], SiO_2 has been found to only interact weakly [23]. Since SMSI is mainly associated with reducible supports [24–26], it can be concluded that whilst the reducible supports (CeO_2, TiO_2 and SnO_2) in this study interacted strongly with the Pt metal, the non-reducible SiO_2 and Al_2O_3 supports only interacted weakly with Pt. Based on the fact that the Pt/SiO_2 catalyst (with weak MSI) was the most active while Pt/CeO_2 (with strong MSI) presented the lowest naphthalene oxidation performance, it can be postulated that SMSI was detrimental to the performance of Pt-supported catalysts in naphthalene oxidation. Pt can interact with reducible supports by forming strong Pt–O–M bridges. For instance, it has been shown [22] that Pt interaction with CeO_2 results in the formation of a Pt–O–Ce bond, *i.e.* MSI which acts as an anchor and inhibits the sintering of Pt particles, thus favoring high dispersion. In the same study [22], Pt was found to interact weakly with Al_2O_3, resulting in mobility and sintering of Pt particles on the surface of the Al_2O_3 support. Hence, it can be concluded that MSI in the present work affected the metal dispersion and average particle size, which was crucial for naphthalene oxidation. In addition to having an effect on Pt distribution, SMSI could also affect the electronic nature of the support and/or Pt and the ease of oxygen mobility. Since the oxidation of naphthalene over Pt-supported catalysts is known to occur by the Langmuir-Hinshelwood mechanism [8] or the Eley-Rideal mechanism [12], it is likely that SMSI could be detrimental to the adsorption and/or diffusion of naphthalene and/or O_2 on the surface of the catalyst.

In order to obtain information about the Pt oxidation state in these catalysts they were analysed using XPS. Fig. 4A shows the Pt(4f) spectra obtained; also indicated on the figure are the expected binding energy values for Pt^0, Pt^{2+} and Pt^{4+} species [27]. There is a wide variation in the intensity and position of component bands between the different catalysts (note that the Pt/Al_2O_3 spectrum is dominated by the Al(2p) core-level peak), but only with Pt/SiO_2 is there any evidence for intensity at the binding energy corresponding to Pt^0. This is highlighted in Fig. 4B where the Pt(4f) spectrum for Pt/CeO_2 has been subtracted from the spectrum for Pt/SiO_2, in order to remove the Pt^{2+} component. The resulting spectrum consists of two doublets corresponding to Pt^0 and Pt^{4+}.

These observations are consistent with the reports of Yazawa et al. [28] and Yoshida et al. [29] who showed that the oxidation state of Pt in Pt-supported catalysts was strongly dependent on the nature of the support, and that the activity for propane combustion [28] and selective reduction of NO by H_2 [29] depended on the oxidation state of Pt. The occurrence of Pt in the metallic form was fostered by the use of acidic supports like SiO_2 as opposed to basic supports like MgO. Metallic Pt proved to be more active in both reactions than oxidized Pt, in agreement with the observations reported here, where the most

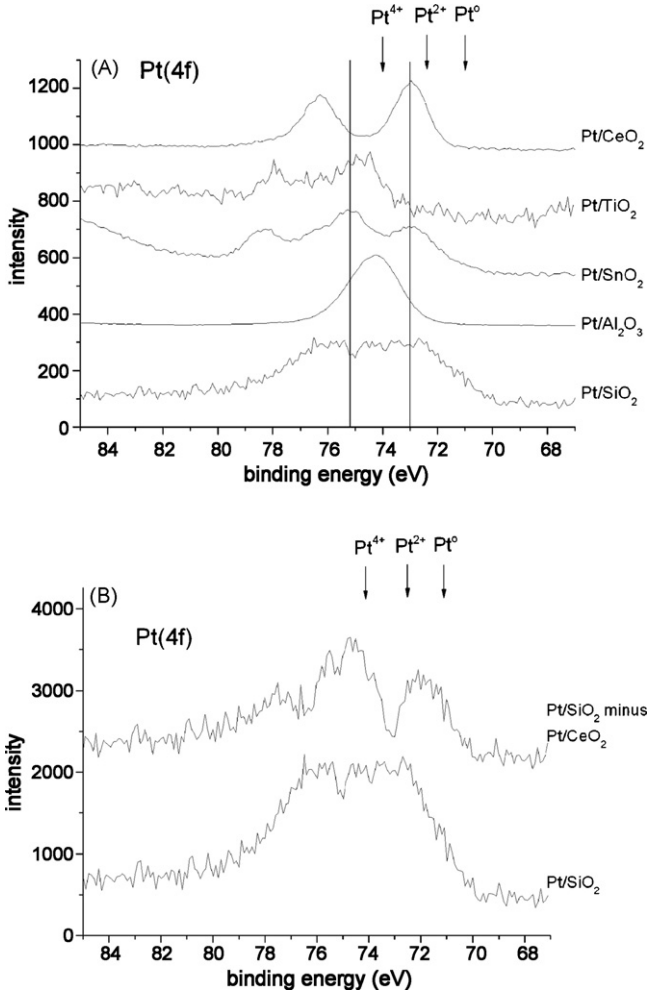

Fig. 4. X-ray photoelectron spectra of Pt-supported catalysts; (A) Pt(4f) core-level spectra for catalysts, as indicated on the figure. Also indicated are the binding energies expected for different Pt oxidation states [27]; (B) Pt 4f) spectrum for the Pt/SiO_2 catalyst, and the resulting difference spectrum after subtraction of the Pt(4f) spectrum for the Pt/CeO_2 sample (which exhibits just Pt^{2+} species).

active catalyst (Pt/SiO_2) contains appreciable amounts of Pt^0. In contrast, oxidized Pt only is present in catalysts supported on less acidic and more reducible supports such as CeO_2, TiO_2 and SnO_2. The basic and redox properties of supports in the latter enhance the presence of oxidized Pt and hence contribute to the lower naphthalene oxidation performance of these catalysts relative to the Pt/SiO_2 and Pt/Al_2O_3.

4. Conclusions

Pt-supported catalysts prepared by impregnation of a variety of support materials (TiO_2, SnO_2, CeO_2, Al_2O_3 and SiO_2) with equal loadings of Pt (0.5%) have been tested for the complete oxidation of naphthalene. The $0.5\%Pt/SiO_2$ catalyst showed considerably higher naphthalene oxidation efficiency than all other Pt-supported catalysts (CO_2 yield of over 50% at 100 °C and over 90% at 200 °C). The differences in the performance of the Pt-supported catalysts have been related to differences in metal dispersion, SMSI (strong interaction between Pt metal and

support) and the oxidation state of Pt, which all depended on the nature of support employed. Large Pt particles (low Pt dispersion) and a weak Pt-support interaction favored naphthalene oxidation. XPS analysis confirms the presence of Pt in the metallic state for Pt/SiO_2 which is likely to be correlated with the superior oxidation performance of this catalyst. Furthermore, the Pt/SiO_2 catalyst showed stable performance with time-on-stream and after temperature cycling.

Acknowledgement

Stuart Taylor and Edwin Ntainjua wish to thank the School of Chemistry, Cardiff University, for funding.

References

[1] B.J. Finlayson-Pitts, J.N. Pitts Jr., Chemistry of the Upper and Lower Atmosphere, first ed., Academic Press, 1999 pp.436–526.
[2] Environment Australia, Technical Report No. 2: Polycyclic aromatic hydrocarbons (PAHs), in Australia, October 1999, ISBN 642547807.
[3] Agency for Toxic Substances and Disease Registry (ATSDR), Atlanta GA: US Department of Health and Human Services, Public Health Service, Toxicology profile for PAHs, 1996.
[4] U.S.E.P.A. (Environmental Protection Agency), Health and Environmental Effects Profile for Naphthalene, EPA/600/x-86/241.
[5] A.K. Neyestanaki, L.-E. Lindfors, Fuel 77 (1998) 1727.
[6] A.K. Neyestanaki, L.-E. Lindfors, T. Ollonqvist, J. Vayrynen, Appl. Catal. A: Gen. 196 (2000) 233.
[7] Z. Xiao-Wen, S.-C. Shen, K. Hidajat, S. Kawi, L.E. Yu, K.Y. Simon, Catal. Lett. 96 (2004) 87.
[8] Z. Xiao-Wen, S.-C. Shen, L.E. Yu, S. Kawi, K. Hidajat, K.Y. Simon, Appl. Catal. A: Gen. 250 (2003) 341.
[9] J. Carno, M. Berg, S. Jaras, Fuel 75 (1996) 959.
[10] F. Klingstedt, A.K. Neyestanaki, L.-E. Lindfors, T. Salmi, T. Heikkila, E. Laine, Appl. Catal. A: Gen. 239 (2003) 229.
[11] M. Ferrandon, E. Bjornbom, J. Catal. 200 (2001) 148.
[12] J.-L. Shie, C.-Y. Chang, J.-H. Chen, W.-T. Tsai, Y.-H. Chen, C.-S. Chiou, C.-F. Chang, Appl. Catal. B: Environ. 58 (2005) 289.
[13] T. Garcia, B. Solsona, S.H. Taylor, Catal. Lett. 105 (2005) 183.
[14] E. Ntainjua N., T. Garcia, S.H. Taylor, Catal. Lett., 110 (2006) 125.
[15] T. Garcia, B. Solsona, S.H. Taylor, Appl. Catal. B: Environ. 66 (2006) 92.
[16] H. Bosch, F. Janssen, Catal. Today 2 (1988) 369.
[17] R. Spinicci, A. Tofanari, Appl. Catal. A 227 (2002) 159.
[18] C.A. Müller, M. Maciejewsky, R.A. Koeppel, A. Baiker, Catal. Today 47 (1999) 245.
[19] K. Sekizawa, H. Widjaja, S. Maeda, Y. Ozawa, K. Eguchi, Catal. Today 59 (2000) 69.
[20] M.S. Waiwright, N.R. Foster, Catal. Rev. 19 (1979) 211.
[21] A. Bossi, F. Garbassi, G. Petrini, J. Chem. Soc., Faraday Trans. 1 (78) (1982) 1029.
[22] Y. Nagai, T. Hirabayashi, K. Domae, N. Takagi, T. Minami, H. Shinjoh, S. Matsumoto, J. Catal. 242 (2006) 103.
[23] R. Burch, P. Fornasiero, B.W.L. Southward, Chem. Commun. (1998) 625.
[24] S.J. Tauster, S.C. Fung, R.L. Garten, J. Am. Chem. Soc. 100 (1978) 170.
[25] S.J. Tauster, Acc. Chem. Res. 20 (1987) 389.
[26] G.L. Haller, D.E. Resasco, Adv. Catal. 36 (1989) 173.
[27] http://www.lasurface.com/database/elementxps.php.
[28] Y. Yazawa, N. Takagi, H. Yoshida, S. Komai, A. Satsuma, T. Tanaka, S. Yoshida, T. Hattori, Appl. Catal., A 233 (2002) 103.
[29] H. Yoshida, M. Hashimoto, J. Shibata, A. Satsuma, T. Hattori, Dep't of Appl. Chemistry, Graduate School of Engineering, Nagoya University, Photon Faraday Activity Report #20 Part B (2003).